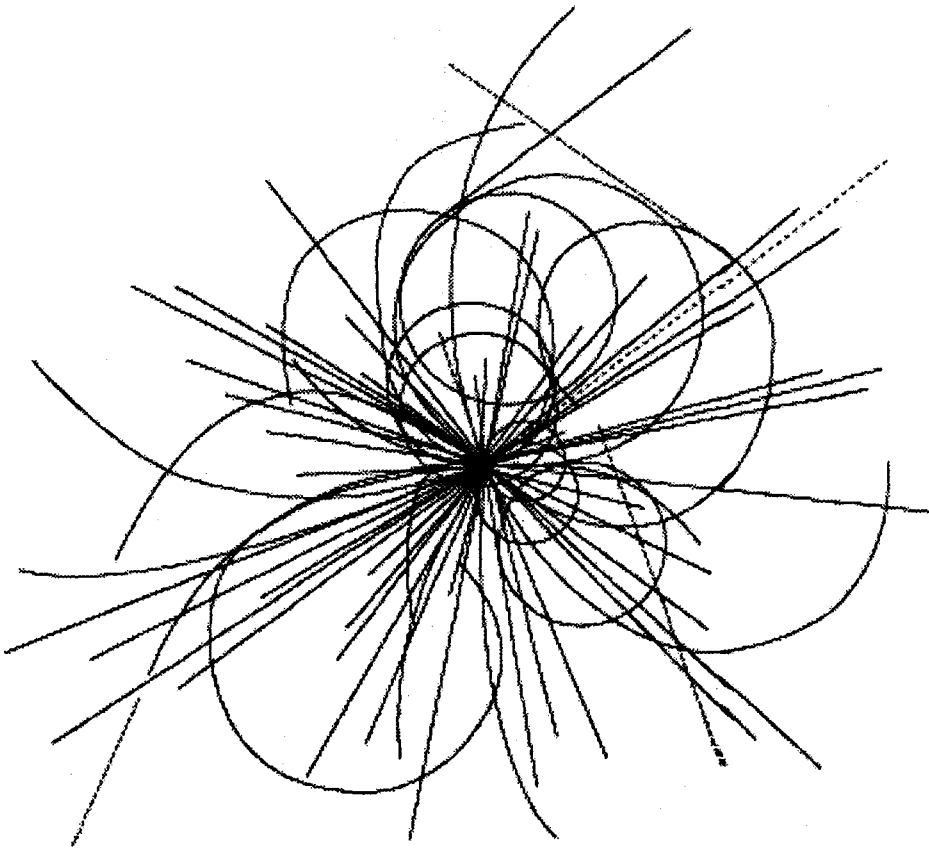


**Electrical Performance Characteristics
of the SSC Accelerator System
String Test**

W. Robinson
W. Burgett
T. Dombeck
J. Gannon
P. Kraushaar
A. McInturff
T. Savord
G. Tool



**Superconducting Super Collider
Laboratory**

**Electrical Performance Characteristics of the
SSC Accelerator System String Test***

W. Robinson, W. Burgett, T. Dombek, J. Gannon,
P. Kraushaar, A. McInturff, T. Savord, and G. Tool

Superconducting Super Collider Laboratory[†]
2550 Beckleymeade Ave.
Dallas, TX 75237

May 1993

*Presented at the 1993 IEEE Particle Accelerator Conference on May 17–20, Washington, D.C.

[†]Operated by the Universities Research Association, Inc., for the U.S. Department of Energy under Contract No. DE-AC35-89ER40486.

ELECTRICAL PERFORMANCE CHARACTERISTICS OF THE SSC ACCELERATOR SYSTEM STRING TEST

W. Robinson, W. Burgett, T. Dombeck, J. Gannon, P. Kraushaar, A. McInturff, T. Savord, and G. Tool
Superconducting Super Collider Laboratory[†]
2550 Beckleymeade Avenue, Dallas, Texas 75237

Abstract

The string test facility was constructed to provide a development test bed for the arc regions of the Superconducting Super Collider (SSC). Significant effort has been devoted to the development and testing of superconducting magnets, spools, and accelerator control systems required for the SSC. The string test facility provides the necessary environment required to evaluate the operational performance of these components as they are configured as an accelerator lens in the collider. This discussion will review the results of high current testing of the string conducted to evaluate magnet element uniformity and compatibility, the splice resistance used to connect the magnets, and system response to various quench conditions. Performance results of the spools, energy bypass systems, energy dump, and the power supply system are also discussed.

I. INTRODUCTION

The intent of the Accelerator System String Test (ASST) is to obtain data for model verification and information on the magnitudes of pressures and voltages encountered in an accelerator environment. The ASST milestone run was accomplished in August, 1992, and consisted of demonstrating that the accelerator components could be configured together as a system operating at full current.^[1] Following the milestone run, the string was warmed to correct some design flaws that limited the operational range. The string was again cooled to cryogenic temperatures in October, and a comprehensive power testing program was conducted through the end of January, 1993. This paper describes how the collider arc components operate in an accelerator environment during quenches induced by firing both strip heaters and spot heaters. Evaluation of the data illustrates how variations in the design parameters of magnets used in a string environment can impact system performance.

II. CONFIGURATION

The ASST is composed of five 50-mm aperture dipole magnets that are 15 meters in length, a five meter long 40-mm aperture quadrupole magnet, and re cooler, feed, and end spools. The dipole magnets used in the string were industrial prototypes constructed by General Dynamics personnel utilizing facilities at Fermi Lab. Those magnets included DCA313, DCA314, DCA319, DCA315, and DCA316. The quadrupole magnet was built at Lawrence Berkeley Lab. The three spool pieces were built to SSCL specification by Meyer Tool (HSPRF), Cryenco (SPR), and Consolidated Vacuum

Industries (HSPRE). A Dynapower Corp. DC current power supply was used to provide a maximum current of 6500 amps. An energy dump was used with the string to evaluate the energy extraction system. A refrigerator with a nominal cooling capacity of 500 watts was used to provide the cryogenics environment. The string cryogenics system is described in another paper presented in this conference.^[2]

Each dipole magnet consists of four superconducting coils. The differential voltage across each coil is monitored by the quench protection monitor system and a data acquisition system. There are four strip heaters for each magnet that are positioned along the length of the outer coils in a quadrant configuration. The strip heaters in opposing quadrants are electrically connected together in parallel. Each set of strip heaters is independently controlled by a heater firing unit. This configuration protects the magnet by providing a level of redundancy that ensures the outer coils quench despite a failure that may occur in one of the heaters or firing units.

Figure 1 illustrates the electrical configuration of the string. In order to reduce the amount of inductance in the system, each half cell is composed of two independent circuits. Each circuit is powered using one of two power busses that run through the magnets. The first three magnets are powered from the lower bus. The remaining dipoles and the quadrupole are powered through the upper bus. The lower and upper busses are connected together at the HSPRE. Diodes are connected across each set of dipoles to provide the required isolation between circuits during quenching conditions. When a quenching condition is detected in a magnet, the strip heaters contained in the magnets within the quenching circuit are fired, and the power supply is turned off. The large resistive voltage that develops across the magnet circuit from the propagating quench condition places a forward bias voltage across the diodes. Current that is flowing from the non quenching magnets bypasses the quenching magnets through the lower impedance path offered by the diodes. Approximately one second after the quench is detected, the energy dump switch is opened and energy remaining in the string is dissipated through the energy dump. Energy contained in the quenching portion of the string is dissipated into the cryo system through the magnet coils.

III. ASST TEST SUMMARY

The string was operated at $T = 4.65$ K partly because of the limitations of the cryogenics plant, but also to keep the amount of operating margin in the magnets small. A total of 66 power tests involving the magnets have been conducted from July 9, 1992, through January 29, 1993. Of those tests, 18 were involved in system commissioning, and 13 were strip heater and spot heater quench tests. One test was the Congressionally mandated milestone demonstration test.^[1] The remainder of the tests involved energy dump testing or

[†]Operated by Universities Research Association, Inc., for the U.S. Department of Energy under Contract No. DE-AC35-89ER40486.

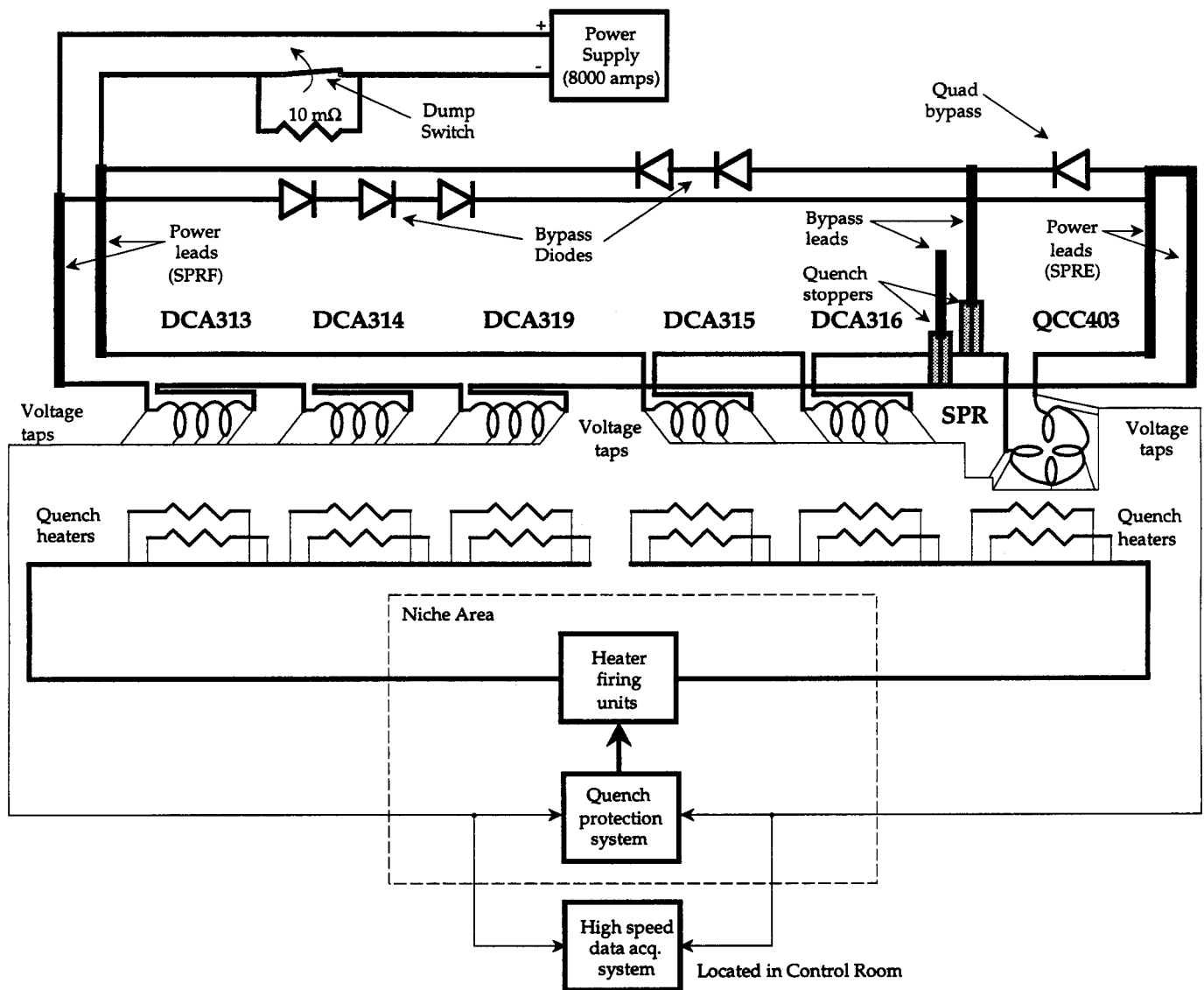


Figure 1. Electrical configuration of the ASST.

bypass lead testing. The opportunities to conduct quench testing were limited because it took the cryogenics system three to four days to recover from a full current quench test. In addition to quench testing, resistance of four splice joints as a function of current were measured.

A. Quench Analysis

Peak voltage in the ASST string configuration is of concern because the dielectric strength of the components in the system must be able to withstand this voltage. The peak voltage is influenced by several factors including the method of quench initiation, circuit inductance, string temperature, and differences in the low temperature (non superconducting) resistance between magnets.

Strip heater induced quenches generate higher voltages than spot heater quenches because a larger segment of one

magnet goes resistive in a shorter period of time. The time rate of resistance growth (dR/dt) is increased in a strip heater induced quench due to the joule heating of the outer coils, while other magnets in the same circuit remain in a superconducting state. Energy from the other magnets supplies energy to the quenching magnet. By the time the other magnets in the circuit quench, the dR/dt of those coils is much lower than in the magnet initiating the event.

Operation at lower temperatures increases the operating margin of the magnets. Once a quench is detected by the quench protection system and the heaters are fired in the other non quenching magnets, the time it takes these magnets to reach a normal state is increased due to the additional operating margin. Meanwhile, the quenching magnet that initiated the event continues to build resistance from joule heating.

One of the unexpected results from testing was the effect that differences in the residual resistivity ratio between

magnets had on the system quench response. (The residual resistivity ratio, or RRR, is defined as the 300 K resistance divided by the 10 K resistance.) Problems were encountered during string testing from using magnets with different RRR values in the same circuit. Table 1 outlines the RRR characteristics of the dipole magnets used in the string. From Figure 1, DCA313, DCA314, and DCA319 are grouped together electrically, and DCA315 and DCA316 are wired together. Some magnets in the circuit were dissipating more of the stored energy at a high rate, while other magnets transferred much of their stored energy to the magnets with lower RRR. Figure 2 illustrates the MIITs (millions of amps squared integrated over time) and peak voltage to ground that were attained during strip heater induced quenches on DCA319. The test was terminated at 6000 amps because the voltage was projected to reach 2300 volts at 6500 amps.

RRR VALUES of ASST MAGNETS

Magnet	UI RRR	UO RRR	LO RRR	LI RRR
DCA313	170	174	171	173
DCA314	174	177	174	171
DCA319	105	96	97	108
DCA315	162	173	174	177
DCA316	67	109	109	78

Table 1. UI is the upper inner coil, UO is the upper outer coil, LO is the lower outer coil, and LI is the lower inner coil.

Volts to Ground and MIITs vs Quench Current

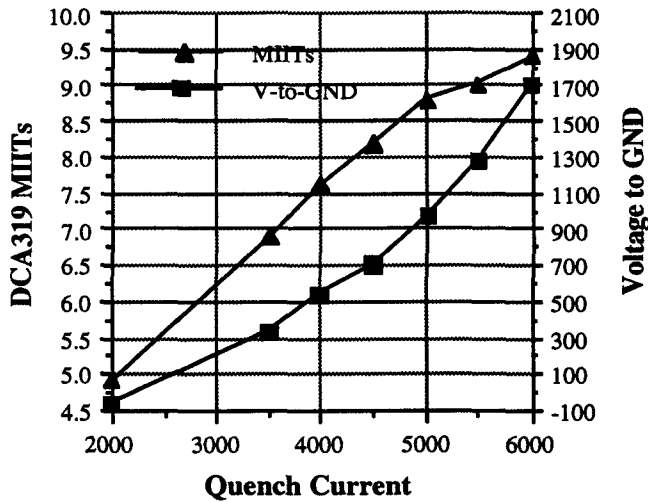


Figure 2. MIITs and voltage to ground as a function current when initiating a string quench by firing the strip heater in DCA319 (T = 4.65 K).

Using the MIITs integral to quantify energy dissipation into heat, it is seen that RRR has an important role in determining the response of the system. The MIITs is determined by

$$MIITs = 10^{-6} \int_0^{\infty} i^2(t) dt = 10^{-6} A^2 d \int_{T_0}^T \frac{C(T)}{\rho(T, RRR, B)} dT,$$

where i is the current, A is the cross-sectional area, d is the density, C is the heat capacity of the conductor, B is the magnetic field term for the magneto-resistance, and ρ is the electrical copper resistivity. An approximation for ρ is

$$\rho(T, RRR) = \frac{1.545}{RRR} + \left(\frac{2.32547 \times 10^9}{T} + \frac{9.57137 \times 10^5}{T} + \frac{.62735 \times 10^{-2}}{T} \right)^{-1} \mu\Omega\text{-cm}.$$

The parenthesis on the right is an approximation to the Grüneisen integral formula for the phonon scattering resistivity.[3] As the RRR of the material is uniformly reduced, its copper resistivity at low temperatures is increased. The MIITs are reduced because the effective time constant of the system is shorter. Stored energy in the magnets dissipates more rapidly when the cold resistivity of the material is higher. Since the resistivity is increased, the peak voltage attained during quench also increases. In a string environment, quenching magnets with lower RRR experience higher MIITs, voltages, and temperatures than anticipated. These higher values are due to the additional energy dissipated in those magnets that is provided from magnets in the system with higher RRR.

Energy deposition estimates were made using the coil voltage $V_c(t)$, which is a combination of the inductive voltage that results from change in current in a coil of inductance L_c , and a resistive voltage resulting from current passing through the copper in the composite superconducting wire. The developed coil resistance $R_c(t)$ is given by

$$R_c(t) = \frac{\left(V_c(t) - L_c \frac{di}{dt} \right)}{i(t)},$$

where di/dt is calculated from the current decay of $i(t)$. Given the resistance of each coil, an estimate is made on how the energy is being dissipated in the string. The total energy stored in the string is given by $W_L = \frac{1}{2} L I_o^2$, where L is the string inductance (approximately 75 mH/dipole and 7.5 mH/quadrupole), and I_o is the string current before a quench occurs. For $I_o = 6500$ amps, the energy storage in the string is $W_L \approx 8$ MJoules. The energy deposition for each coil is determined by

$$W_{R_c} = \int_{t_0}^{\infty} R_c(t) i^2(t) dt,$$

where t_0 represents when resistance in the coil is detected.

Figure 3 illustrates how the string energy is dissipated in the string during Event #285 when all strip heaters are fired simultaneously. DCA319 dissipated the most energy because it had the lowest RRR of the three dipoles in its circuit (see Figure 1). Although the RRR of DCA316 is similar to DCA319, there was only one other dipole in the DCA316 circuit. The total energy dissipated by Event 285 was 7.79 MJoules. The 3.68% difference from the expected energy of 8.08 MJoules is due to the change in the dipole inductance from the high field iron core saturation.

Energy Dissipation Profile for Event 285

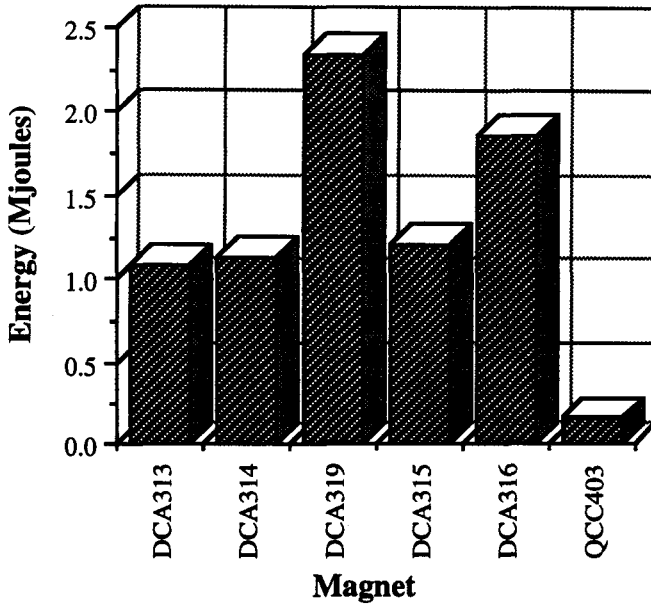


Figure 3. Profile of energy dissipation for Event 285 where all strip heaters were fired simultaneously. Peak current for this event was 6475 amps.

C. Ramp Rate Study

Significant effort has been expended on understanding dipole ramp rate sensitivity during single magnet testing. The test facility at used at FNAL did not have an energy dump and was unable to conduct decay ramp sensitivity tests. The baseline dump resistance used in the ASST was increased from 10 mΩ to 16 mΩ in order to reduce the time constant of the system. Table 2 summarizes the result of the test.

Event #	Dump Ω	di/dt [amps/sec]
359	10 mΩ	237.2
375	12 mΩ	276.0
369	16 mΩ	339.3

Table 2. Ramp rate sensitivity tests. DCA313 and DCA315 quenched at 5300 amps during Event 369.

During energy dump using a dump resistance of 16 mΩ, dipole magnets DCA313 and DCA315 quenched due to eddy current heating. Of the magnets used in the string, DCA313 and DCA315 exhibited the highest sensitivity to di/dt during single magnet testing.^[4] It is possible that if we were operating the string at 4.35 K, we would have been able to successfully dump the system using the 16 mΩ dump impedance without quenching.

Calculations to estimate the resistance change required to obtain a desired ramp rate were performed. The relationship for estimating resistance is

$$R = -\frac{L}{t} \ln \left(1 - t \frac{\left(\frac{di}{dt} \right)}{I_0} \right),$$

where L is the system inductance of 382.5 mH, di/dt is the desired ramp decay in amps/sec, t is the time interval, and I_0 is the initial current. Since the initial decay rate at $I_0 = 6500$ amps for a dump resistance of 10 mΩ was 237.2 amps/sec, the system load including the power bus resistance is calculated to be 14.8 mΩ. Assuming the incremental change in the dump resistance is accurate, the above equation can be used to solve for system inductance. Changing the system load impedance by 2 mΩ, the inductance is 368 mH. Increasing the load resistance by 4 mΩ, the system inductance is approximately 367 mH. The percent change in inductance of 3.79% is consistent with results from the joule deposition calculation presented in the previous section. Using the new inductance in the above equation leads to a system impedance of 14.24 mΩ when using the 10 mΩ dump resistance.

D. Spot Heater Testing

The limited operations schedule permitted only two spot heater tests at the full current of 6500 amps. We induced full current spot heater quenches on DCA313 and DCA319. This provided a comparison for voltage to ground and MIITs development between dipole magnets of different RRR values (see Table 1). Table 3 summarizes the comparison between DCA313 and DCA319 as well as lower current spot heater tests conducted on DCA319. As expected, the maximum MIITs developed on DCA319 occurred below 6500 amps.

Magnet	Max current	Volts to GND	MIITs
DCA313	6500	566	11.55
DCA319	6500	1232	10.99
DCA319	6000	923	11.3
DCA319	5000	418	10.95

Table 3. Spot heater test results.

An unexpected event occurred during the spot heater test conducted on DCA313 that was similar to a full current strip heater quench conducted earlier on the same magnet (Event 335). Normally when a quarter cell quenches, the heat from the quench propagates into the magnet in the adjoining quarter cell causing a thermally induced quench. We ordinarily would have expected DCA315 (in the fourth dipole position) to experience a thermal quench. In both cases, when DCA313 was quenched at full current, DCA316 (in the fifth dipole position) experienced a thermal quench. One possible cause could be heating from the re cooler in the SPR due to the differential pressure that develops from the induced cryogenic flow impedance. We currently do not have enough data to accurately characterize this process.

E. Bypass Lead Testing

The bypass leads located on the SPR are composed of stainless steel that are used to conduct current from the superconducting power bus to the outer cryostat during quenching conditions. The stainless steel is used to provide thermal isolation without excessive heat leak into the cold mass. Since stainless steel is a relatively poor electrical conductor, care must be taken not to overheat the lead during

operation. The lead must be designed to withstand the MIITs developed during an energy dump which is determined by

$$MIITs = 10^{-6} \int_0^{\infty} i^2(t) dt = 10^{-6} \int_0^{\infty} \left(I_0 e^{-\frac{Rt}{L}} \right)^2 dt = \frac{I_0^2 L}{2R} \times 10^{-6}.$$

For the Collider, the maximum operating current is $I_0 = 7$ kA, the circuit inductance is 39 H, and the dump resistance is approximately 1Ω . The MIITs requirement for the bypass lead is 1000 MIITs. We conducted a series of experiments designed to evaluate bypass lead performance. The lower bypass lead was tested to 1400 MIITs, and the upper bypass lead was tested to 2040 MIITs.

F. Splice Joint Resistance

Voltage taps were placed on each side of four splice joints in the string. The voltages across the joints were monitored while ramping the string to full current. Figure 4 illustrates the splice joint resistances from 2000 amps to the full current of 6500 amps. These were also the first joints fabricated in the field so it is expected that the impedance will become lower as our processes continue to improve and experience is gained in joint fabrication. The change in resistance as a function of current is due to the superconducting properties of solder at low currents. The differences between splice impedance at high current is probably due to differences in the solder composition or thickness between joints. The thickness can be thought of as the distance between superconducting composite strands in the opposite sides of the joint with respect to each other.

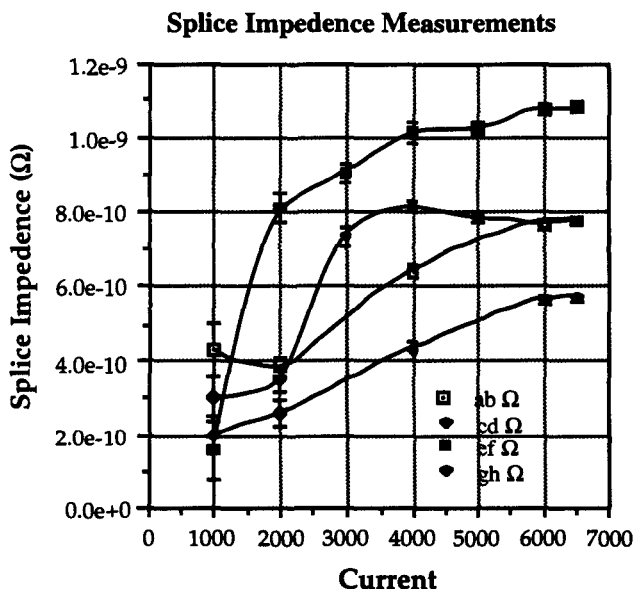


Figure 4. Splice joint resistance as a function of current. The "hump" in the "gh Ω " curve is probably due to measurement error.

IV. FULL CELL RUN

We are currently reconfiguring the string as a full cell that is scheduled for cool down sometime in July. The full cell is composed of 10 dipole magnets and two quadrupole magnets. The dipole magnets are grouped together based on RRR into four families. We expect the energy dissipation of the system to become more balanced as each RRR family is configured together through one bypass circuit. The full cell will be operated utilizing one of the sector refrigerators that has been built for the Collider. The refrigerator will permit operation at lower temperature, and will recover from a full power quench in a much shorter time than the refrigerator used previously. We plan to continue monitoring splice joint resistance and to conduct studies on power bus quenches. A fully instrumented SPR will replace the original SPR. The additional instrumentation allows us to study quench dynamics between half cells. The corrector package in the SPR is operational. The additional instrumentation in the SPR may also allow us to understand how a full current quench in the first dipole induces a thermal quench in the dipole adjoining the SPR.

V. CONCLUSIONS

Important progress has been made on the Collider design in the past two years. We have identified several problems early enough in the design cycle to have significant impact. With the exception of the problem encountered in matching RRR values between dipoles, we have not encountered any operational problems that would prohibit full current operation of the Collider. The problem encountered with RRR matching is currently being addressed at the design level, and will be solved before magnet production for the Collider has begun.

VI. ACKNOWLEDGMENTS

The authors wish to recognize the excellent work and significant contribution the many groups and individuals that supported the design, integration, and operations expertise. The string assembly crew led by C. White, the cryogenics crew led by R. Ahlman, and the operations team led by M. Hentges deserve special recognition for their dedicated effort and professional performance.

VII. REFERENCES

- [1] W. Burgett, et al., "Full-Power Test of a String of Magnets Comprising a Half-Cell of the Superconducting Super Collider," SSCL-Preprint-162, October, 1992. (To be published in the journal *Particle Accelerators*.)
- [2] A. McInturff, et al., "Collider Scenario Implications of ASST Operation," Paper Jc4 of the *1993 Particle Accelerator Conference*, Washington D. C., May, 1993.
- [3] M. McAshan, "MIITs Integrals for Copper for Nb-46.5 wt% Ti," SSC-N-468, February, 1988.
- [4] J. Kuzminski, et al., "Quench Performance of 50-mm Aperture, 15-m-Long SSCL Dipole Magnets Built at Fermilab," SSCL-Preprint-133, presented at *The XVth International Conference on High Energy Accelerators*, Hamburg, Germany, July, 1992.